

POINT POSITIONING ACCURACY OF AIRBORNE LIDAR SYSTEMS: A RIGOROUS ANALYSIS

Nora Csanyi May^{1,2*}, Charles K. Toth²

Department of Civil and Environmental Engineering and Geodetic Science¹
Center for Mapping²
The Ohio State University
1216 Kinnear Road, Columbus OH 43212-1154, E-mail: nora@cfm.ohio-state.edu

Commission I, WG I/2

KEY WORDS: Airborne LiDAR, Accuracy Analysis, Error Propagation, Error Sources, Multi-Sensor Systems, GPS/INS

ABSTRACT:

This paper provides a comprehensive analysis of the achievable point positioning accuracy for airborne LiDAR systems considering all the major potential error sources. Using the law of error propagation, rigorous analytical derivation of error formulas was performed to obtain a reliable assessment of the achievable point positioning accuracy. For practical use, based on the derived analytical formulas, accuracy figures and tables have been developed. In this paper select example figures illustrate the achievable point positioning accuracies of state-of-the-art LiDAR systems for various accuracies of the parameters that influence the LiDAR point positioning accuracy. The analytical derivation-based accuracy plots can also be used as a tool for choosing the right system or system configuration for a desired mapping accuracy, and to help the flight planning, i.e. selecting optimal flight parameters for a given system to achieve the desired point positioning accuracy. In addition, the developed error formulas can also facilitate the analysis of the effects of individual error sources on point positioning accuracy, although due to the size limitations of the paper this analysis is not included in this paper.

1. INTRODUCTION

LiDAR systems are complex, multi-sensor systems consisting of at least three sensors, the GPS and INS navigation sensors, and the laser scanner system. Consequently, proper system calibration, including individual sensor calibration, inter-sensor calibration, and time synchronization between system components is crucial in achieving the required mapping accuracy. Furthermore, besides errors in the calibration parameters, there are several other error sources that can degrade the accuracy of the derived ground coordinates, such as, for example, errors in the navigation solution (position and attitude errors), range measurement errors, etc. In addition, the effect of the various errors is influenced by the various flight parameters (flying height, flying speed, etc.), terrain characteristics, and system settings, and accordingly, the dependency of point positioning accuracy on the various error sources is very complex. As a consequence, the reliable accuracy assessment and performance validation of the derived mapping products is a very challenging task.

Most publications, discussing the effects of different error sources on the point positioning accuracy of LiDAR systems typically focus on a single or a few error sources and do not discuss the combined effect of all error sources. Baltsavias (1999), for example, provides an overview of basic relations and error formulas concerning airborne laser scanning. Schenk (2001) provides a summary of the major error sources for airborne laser scanners and error formulas focusing on the effect of some systematic errors on point positioning. A number of papers empirically evaluates the achieved accuracy of specific

mapping projects, normally using ground control as reference (Latypov, 2002; Hodgson and Bresnahan, 2004; Hodgson et. al., 2005; Peng and Shih, 2006). LiDAR vendors provide specifications on the approximate accuracy that can be expected from their systems. These values, however, are mostly valid under specific circumstances (for specific flying height, GPS baseline, etc.), and only consider a few error sources, and consequently are frequently either too optimistic or too pessimistic. Furthermore, some of the vendors do not clearly state what error sources are considered when they provide the accuracy specifications, which makes it difficult and, in some cases, nearly impossible to compare the achievable accuracies of different systems from different vendors. For example, some LiDAR vendors specify the achievable point accuracy considering the GPS errors, while others do not include this error in their accuracy specifications. In conclusion, no generally accepted, comprehensive and reliable accuracy assessment tool exists to help with flight or project planning in order to achieve the desired accuracy of the final product of LiDAR systems.

This paper is intended to fill the void by providing a comprehensive accuracy assessment tool for airborne LiDAR systems that considers all the major potential error sources, and consequently a reliable assessment of the achievable point positioning accuracy can be obtained. The first section of the paper provides an overview of the analytical derivation of the error formulas. In the second section, example plots of the achievable point positioning accuracies of different systems for various accuracies of the parameters that influence the point positioning accuracy are shown and analyzed.

* Corresponding author.

2. RIGOROUS ERROR PROPAGATION

To reliably determine the achievable point positioning accuracy of airborne LiDAR systems, all the major potential error sources that influence the point positioning accuracy have to be considered in the analytical derivations. The random errors listed in Table 1 were considered during the analytical derivations. The 2nd column of Table 1 also shows the symbols for the respective standard deviation values as used in this paper; the laser beam divergence (γ) itself is obviously not an error term, however, its effect, the finite footprint size represents an additional random error source.

Error source	Used symbol
Navigation solution errors	
Position errors	$\sigma_X, \sigma_Y, \sigma_Z$
Attitude angle errors	$\sigma_\omega, \sigma_\phi, \sigma_\kappa$
Errors in the determined boresight misalignment angles	$\sigma_{\omega_b}, \sigma_{\phi_b}, \sigma_{\kappa_b}$
Range measurement error	σ_r
Scan angle error	σ_β
Laser beam divergence	γ

Table 1. Considered error sources

The error formulas for point positioning accuracy were derived based on the LiDAR equation (Eq.1.) via rigorous error propagation, see also Figure 1.

$$r_M = r_{M,INS} + R_{INS}^M (R_L^{INS} \cdot r_L + b_{INS}) \quad (1)$$

where

- r_M — 3D coordinates of object point in the mapping frame
- $r_{M,INS}$ — Time dependent 3D INS coordinates in the mapping frame, provided by GPS/INS (refers to the origin of the INS body frame)
- R_{INS}^M — Time dependent rotation matrix between the INS body and mapping frame, measured by INS
- R_L^{INS} — Boresight matrix between the laser frame and INS body frame
- r_L — 3D object coordinates in laser frame
- b_{INS} — Boresight offset vector

Using the law of error propagation based on the covariance matrix of the error sources listed in Table 1, the covariance matrix of the 3D LiDAR positions was derived as described in Eq. 2.

All analytical derivations were implemented in MATLAB environment; due to size limitations of this paper, the derived formulas are not shown here. The effect of laser beam divergence was considered separately from the error propagation (but later combined) since the horizontal error due to the footprint size can be characterized by uniform distribution instead of the normal distribution. Furthermore, the boresight offset component was assumed to be error free since its effect is negligible, as compared to the effects of other errors.

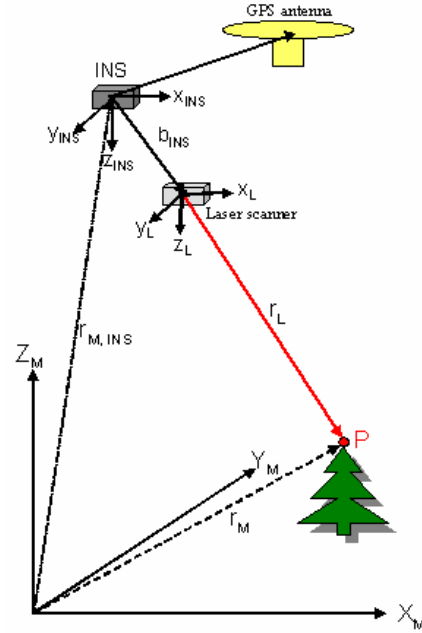


Figure 1. LiDAR system components and definitions.

$$C_{LiDAR} = ACA^T \quad (2)$$

where

- C_{LiDAR} [3x3] — Covariance matrix of the LiDAR point coordinates
- C [11x11] — Covariance matrix of the INS position, INS attitude angles, boresight angles, measured range, and the scan angle
- A [3x11] — Jacobean matrix containing the partial derivatives of X,Y, Z LiDAR coordinates with respect to the different random variables in the LiDAR equation

The following assumptions were made during the analytical derivations: Flat terrain was assumed, sloped terrain will cause additional errors in the vertical coordinates as compared to the error propagation results; however, this effect can easily be considered and accounted for separately. The error formulas were developed considering that the scanning is performed in a vertical plane perpendicular to the flight direction. The range measurement accuracy is assumed to be independent of the flying height and scan angle, which for earlier systems was not exactly the case, since longer range due to higher flying height and larger scan angle meant weaker signal response, and consequently less accurate range measurement. However, according to LiDAR vendors, for the state-of-the-art systems, the range measurement accuracy does not noticeably degrade for longer ranges. During the derivations the various errors mentioned above were considered to be uncorrelated with each other, however, any correlation between variables could easily be considered by changing the covariance matrix to non-diagonal.

Using the derived error formulas, based on the accuracy of the parameters listed in Table 1, the achievable point positioning accuracy can be computed for any given LiDAR system operated at different flying heights, etc.

3. EXAMPLES OF ACHIAVABLE LIDAR POINT POSITIONING ACCURACY

In the following examples, select accuracy plots are shown. The figures were generated using typical accuracy values for the various error sources that represent the state-of-the-art LiDAR systems. For the flight parameters, such as flying height, and the maximum scan angle values – or in some figures value ranges – that are frequently used in LiDAR mapping, were considered.

The accuracy of the navigation parameters, the position and attitude angle accuracies used in these examples are chosen based on the post-processed accuracy specifications of the Applanix POS/AV™ systems. Since the examples are intended to illustrate the performance that can be expected from state-of-the-art systems, only the accuracies provided by the high-end systems, such as POS/AV™ 410-610, (www.applanix.com) were considered for the examples. Consequently, for the generation of the following accuracy plots, the accuracy ranges listed in Table 2 were used. For the accuracy of the boresight misalignment angles, typical achievable standard deviations of the calibrated boresight misalignment angles were considered (Burman, 2001; Skaloud and Lichti, 2006). Table 2 contains the values that were used in the generated examples. The range measurement was assumed to have a 1 cm standard deviation (1σ), this value is based on the system specifications of state-of-the-art LiDAR systems. It should be emphasized that our example plots assume hard surfaces; the ranging accuracy used in our computations is obviously not valid in vegetated areas. The accuracy of scan angle measurement is typically not addressed in the literature or in the system specifications provided by LiDAR vendors. In the examples below, a quantization error with 0.0007° standard deviation (1σ) was assumed, which was mentioned as a valid value for the Riegel LMQ-280 system in (Campbell, et. al, 2003). The laser beam divergence (γ) of 0.3 mrad was considered based on LiDAR system specifications of modern LiDAR systems.

Parameter	Value (1σ)
σ_X, σ_Y	5-15 cm,
σ_Z	7.5-22.5 cm ($1.5 \cdot \sigma_X, \sigma_X = \sigma_Y$)
$\sigma_\omega, \sigma_\phi$	10"-30"
σ_κ	20"-60" ($2 \cdot \sigma_\omega, \sigma_\omega = \sigma_\phi$)
$\sigma_{\omega_b}, \sigma_{\phi_b}$	10"
σ_{κ_b}	30"
σ_r	1 cm
σ_β	0.0007°

Table 2. Standard deviation values of parameters assumed for the illustrated examples

For the sake of simplicity, the plots below illustrate the accuracy of the LiDAR point coordinates in a local right-handed coordinate system that has its X-axis aligned in the flight direction, Y-axis points to the scan direction, and Z up. Furthermore, for the generation of these plots all three aircraft attitude angles (roll, pitch, and heading) were assumed to be zero for the same reason, but any other value could be used in the derived accuracy formulas. In all plots shown in the paper the vertical (Z) accuracy is shown in red, the accuracy in the scan direction (Y) is marked with green color, and in the flying direction (X) it is shown in blue.

3.1 The Effect of Attitude Angle Errors

Figure 2 and 3 illustrate the effect of attitude angle errors on the achievable point positioning accuracy as a function of scan angle for 600 m and 1500m flying height, respectively. To better show the effects of the attitude angle errors, in these figures all other variables are considered to be error free. The ‘Sigma omega phi’-axis of these figures show the $\sigma_\omega, \sigma_\phi$ values, the σ_κ value was taken according to the ratio shown in Table 2. As the figures show, the attitude angle errors have stronger effect on the horizontal positions than on the vertical one, and errors in all three coordinate directions increase for higher flying heights. Furthermore, the effect of attitude angle errors on the coordinate accuracy in the scan direction does not change with the scan angle, while the accuracy in both the flying direction and the vertical coordinate direction degrades with increasing scan angles (towards the sides of the LiDAR strips). This increasing effect of attitude angle errors in the flying direction is caused by the κ angle error that has increasing effect for larger scan angles, while the accuracy degradation of the vertical coordinates towards the sides of the strip is due to the ω attitude angle error that also has increasing effect with larger scan angles.

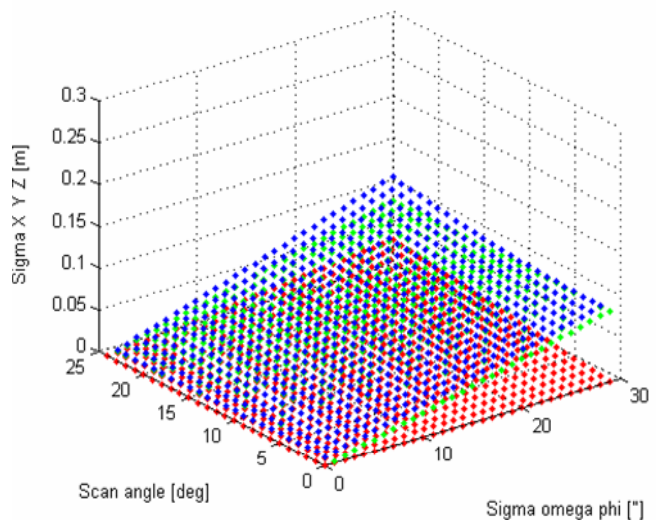


Figure 2. Effect of attitude angle errors on point positioning as a function of scan angle for H=600 m.

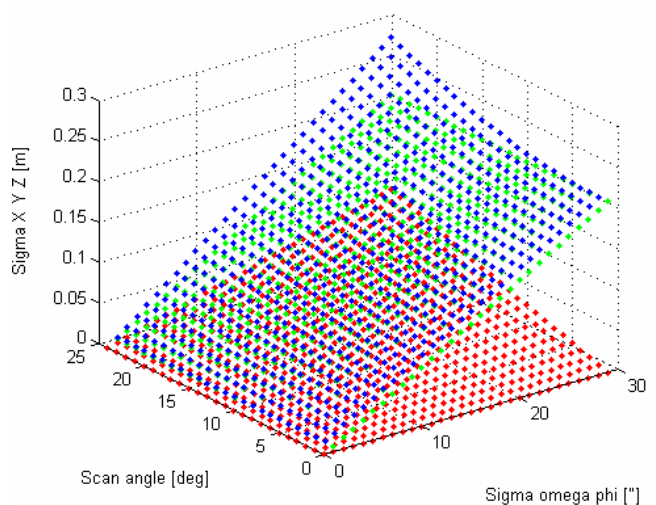


Figure 3. Effect of attitude angle errors on point positioning as a function of scan angle for H=1500 m.

3.2 The Effect of All Navigation Errors

To illustrate the effect of the accuracy of all the navigation parameters, Figure 4 and 5 illustrate the achievable point positioning accuracy as a function of the accuracy of the aircraft position and attitude angles for 600 m and 1500m flying height, respectively. To better show the effects of navigation errors, in these figures all other variables are considered to be error free. The figures illustrate the point positioning accuracies at 10° scan angle, and in order to also show the effect of aircraft position and the attitude errors separately from each other; the point positioning accuracies were computed starting at zero navigation errors, but the realistic values are in the ranges shown in Table 2. As Figure 4 illustrates, for lower flying heights, the accuracy of the aircraft position has a relatively larger effect on the point positioning accuracy as compared to the angular errors (in particular, on the vertical coordinates). Note that the higher positioning errors in the vertical coordinates for larger aircraft position errors in this figure are caused by the 1.5 ratio of $\sigma_z/\sigma_{X,Y}$ (which is rather realistic) used in the computation. This might be a bit surprising, since LiDAR vertical accuracy is known to be better than the horizontal one, which, as the other figures show, is normally true due to the other errors that affect the horizontal position more (especially the beam divergence and attitude errors). As Figure 5 shows, as the flying height increases, the attitude angle errors have increasing effect on the point positioning accuracy, while the effect of aircraft position errors do not increase.

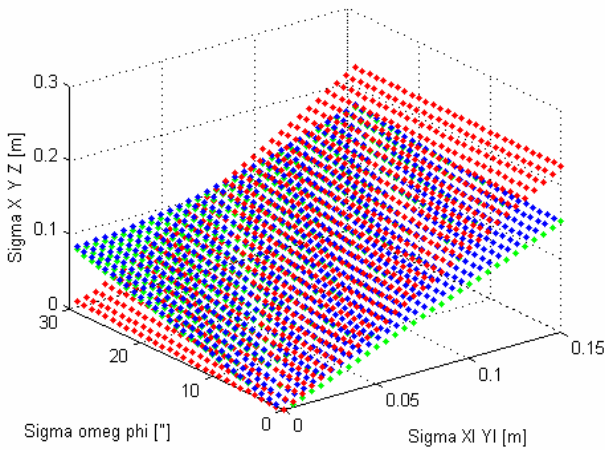


Figure 4. Effect of navigation errors on point positioning for H=600 m at 10° scan angle.

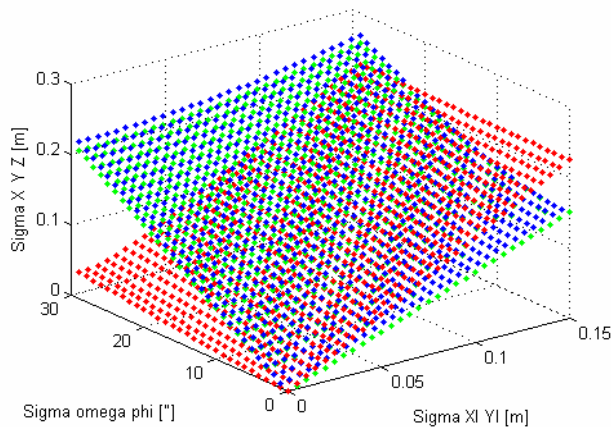


Figure 5. Effect of navigation errors on point positioning for H=1500 m at 10° scan angle.

3.3 All Error Sources Considered

Figure 6 and 7 illustrate the point positioning accuracies for the same cases as Figure 4 and 5, but in these figures all other error sources with accuracies listed in Table 2 were also considered. The zero aircraft position error and zero attitude error (which is obviously not a realistic case) is only intended to show the effect purely of all other error sources excluding the navigation errors. As these plots show, these other error sources have stronger effect on the horizontal position than on the vertical, and especially for higher flying height, the vertical LiDAR point accuracy is indeed better as compared to the horizontal accuracy (except for some unrealistic cases when the accuracy of the aircraft position is much worse than that of the attitude angles).

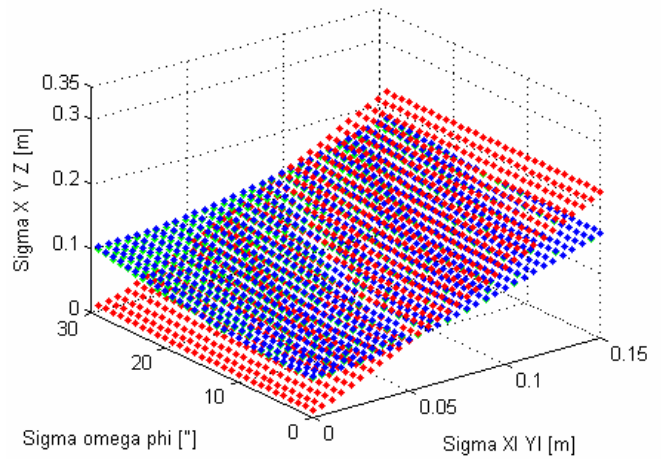


Figure 6. Standard deviation of point positioning for H=600m at 10° scan angle as a function of navigation errors, all errors considered.

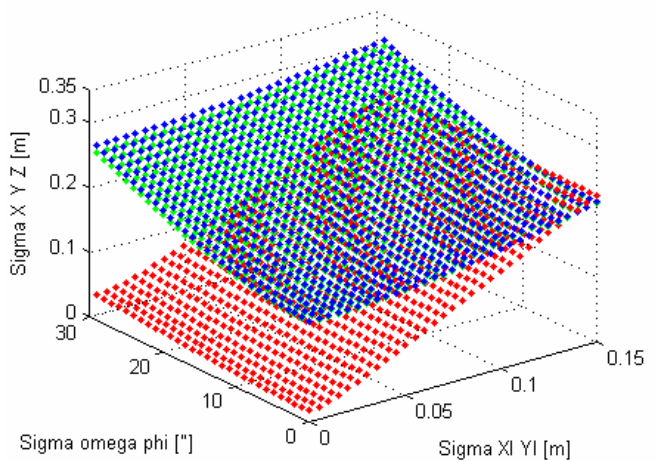


Figure 7. Standard deviation of point positioning for H=1500m at 10° scan angle as a function of navigation errors, all errors considered.

3.4 Flying Height and Scan Angle Dependency

Finally, Figure 8 illustrates the point positioning accuracies achievable as a function of flying height and scan angle. This plot is intended to show the case of a state-of-the-art LiDAR system including a highly accurate navigation solution. For this figure the following standard deviations were considered: $\sigma_x=\sigma_y=5\text{cm}$, $\sigma_z=7.5\text{cm}$, $\sigma_\omega=\sigma_\phi=15''$, $\sigma_\kappa=30''$, the accuracy of the other parameters were assumed as shown in Table 2. As

the figure illustrates, as the flying height increases, the accuracy of the vertical coordinates do not significantly decrease (especially for smaller scan angles), while the horizontal point positioning accuracy does. Towards the LiDAR strip edges (with higher scan angles) all three coordinates show degrading accuracy; in the scan direction this degradation is small, while in the flying direction and vertical direction the errors increase more. The higher degradation in accuracy in the flying direction as compared to the scan direction – that is noticeable in the figure – can be explained by the fact that errors in the heading and in the κ boresight angle affect the accuracy in the flying direction, and this effect significantly increases with higher scan angles.

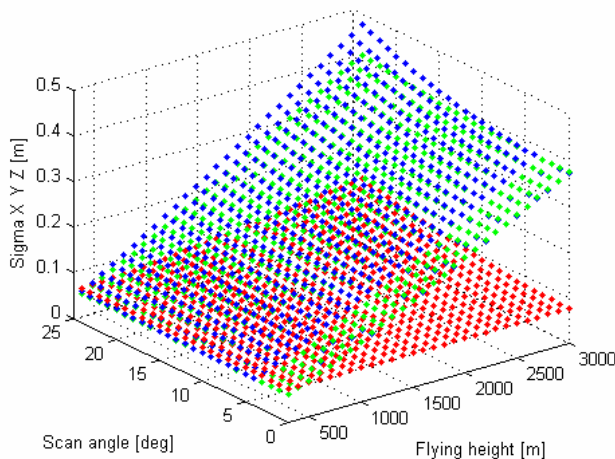


Figure 8. Standard deviation of point positioning as a function of flying height and scan angle, all errors considered.

4. CONCLUSIONS

This paper presented a comprehensive analysis of the achievable point positioning accuracy of airborne LiDAR systems using rigorous analytical derivations via error propagation. LiDAR systems in reality are rather complicated and consequently not all potential error sources could be accounted for in this analysis. However, as all the major error sources were considered, therefore, we believe that for well-calibrated LiDAR systems the derived formulas provide a rather realistic and reliable accuracy assessment when the accuracies of the considered parameters that influence the point positioning accuracy are reasonably well known.

Using the derived error formulas, based on the accuracy of the navigation solution, the boresight misalignment angles, the ranging and scan angle accuracy, and laser beam divergence, the achievable point positioning accuracy can be computed for any given LiDAR system, operated at different flying heights, etc. The accuracy plots that were derived based on the analytical derivations can be used as a tool for choosing the right system for given application requirements, and to help with flight planning to decide on the optimal flying height, and maximum scan angle to achieve the desired point positioning accuracy. Due to the length limitations of this paper, the effects of individual error sources on point positioning accuracy were not analyzed here, but the developed error formulas also facilitate that type of analysis.

5. REFERENCES

- Baltsavias, E.P., 1999. Airborne laser scanning: basic relations and formulas. *ISPRS Journal of Photogrammetry & Remote Sensing* Vol. 54, pp. 199-214.
- Burman, H., 2000b. Calibration and Orientation of Airborne Image and Laser Scanner Data Using GPS and INS, PhD dissertation, Photogrammetry Reports No. 69, Royal Institute of Technology, Stockholm, 107 p.
- Campbell, J. L., M. Uijt de Haag, and A. Vadlamani, 2003. The Application of LiDAR to Synthetic Vision System Integrity, *IEEE Digital Avionics Systems Conference, 2003, DASC '03*, 12-16 Oct. 2003, Vol. 2., pp. 91-97.
- Hodgson, M. E. and P. Bresnahan, 2004. Accuracy of Airborne LiDAR-Derived Elevation: Empirical Assessment and Error Budget, *Photogrammetric Engineering & Remote Sensing*, Vol. 70, No. 3., March 2004, pp. 331-339.
- Hodgson, M.E., J. Jensen, G. Raber, J. Tullis, B. A. Davis, G. Thompson, and K. Schuckman, 2005. An Evaluation of Lidar-derived Elevation and Terrain Slope in Leaf-off Conditions, *Photogrammetric Engineering & Remote Sensing*, Vol. 71, No. 7., July 2005, pp. 817-823.
- Latypov, D., 2002. Estimating relative lidar accuracy information from overlapping flight lines. *ISPRS Journal of Photogrammetry and Remote Sensing*, Volume 56, Issue 4, July 2002, pp. 236-245.
- Peng, M. H. and T. Y. Shih, 2006. Error Assessment in Two Lidar-derived Datasets. *Photogrammetric Engineering & Remote Sensing*, Vol. 72, No. 8, August 2006, pp. 933-947.
- Schenk, T., 2001. Modeling and Analyzing Systematic Errors in Airborne Laser Scanners. *Technical Notes in Photogrammetry*, vol. 19. The Ohio State University, Columbus, USA. 46 p.
- Skaloud, J. and D. Lichti, 2006. Rigorous approach to bore-sight self-calibration in airborne laser scanning. *ISPRS Journal of Photogrammetry & Remote Sensing* Vol. 61, pp. 47-59.